Electrozone Sensing Goes Nano

Margarida Figueiredo, Paulo Ferreira and Elisa J. Campos

University of Coimbra, Coimbra, Portugal

Recent advances in nanopore-based technologies and microelectronics allowed the resurgence of Coulter counter-based techniques. Known collectively as resistive pulse sensing, this technique is now capable of characterizing nanoscale objects, such as nanoparticles, viruses, DNA, and other polymers, while keeping the main attractions of the classical versions: simplicity, sensitivity and resolution, and single-object readout.

Besides an accurate characterization of both size and concentration of the nanoparticles in their natural environment, additional information about particle surface charge is currently possible in an individual basis. Furthermore, efforts have been made to integrate the nanopores in microfluidic systems with the inherent advantages in terms of portability and cost as well as the ability to integrate multiple functions.

This survey aims to review the progress in resistive pulse sensing toward the characterization of submicron particles, with special emphasis on nanopore design (natural and synthetic) and on lab-on-a-chip devices.

1 INTRODUCTION

The electrical sensing zone method, also called resistive pulse sensing, is one the most widely used counting methods, being routinely applied in the medical and industrial fields to determine particle size distribution. It was invented by Wallace Coulter (and for that is frequently known as the 'Coulter principle') for counting blood cells rapidly, in the late 1940s, but was only patented and described in detail in 1953.[1] The Coulter's patent is among only a few patents in science that revolutionized clinical practice to this very day.[2] However, it has become very popular not only for counting and sizing blood and other cells and organisms but also for measuring the size distribution of a wide range of particulate materials as drugs, pigments, fillers, foodstuffs, cosmetics, pharmaceuticals, explosives, minerals, and metals. In fact, characterizing dispersion properties on a particle-by-particle basis can represent a major advantage for investigating and understanding the fundamental behavior of all particulate suspensions.

Details of the Coulter counter working principle to characterize micron-sized particles have been extensively reported in the literature and thus will only be briefly mentioned here.[3-5] As illustrated in Figure 1, particles homogeneously suspended at a low concentration in an electrolyte solution are forced to flow, substantially singly, through a small aperture (that constitutes the sensing zone) in a nonconductive membrane that separates two electrodes of opposite potential. When a particle passes through the aperture, it displaces the conducting electrolyte, increasing the resistance of the aperture. This increase in resistance is known as a *resistive pulse*.

The passage of a number of particles produces a series of pulses (current or voltage) whose amplitudes are essentially proportional to the excluded particle volumes. These pulses are then amplified, sorted, and counted providing information about particle number and size (equivalent volume diameter).[3,4] The measured particle sizes can be accumulated to obtain a particle size distribution. If the volume of liquid passing through the aperture is measured, then the absolute concentration of the sample can be determined. Coulter-type sensors can detect the size of particles with high reproducibility and resolution in a short time (several thousands of particles per second). Although these instruments are still routinely used in research and histology labs, namely speeding up the process of detection and counting blood cells, the large aperture sizes produce unreliable results when analyzing much smaller particles, namely nanometer-scale objects.
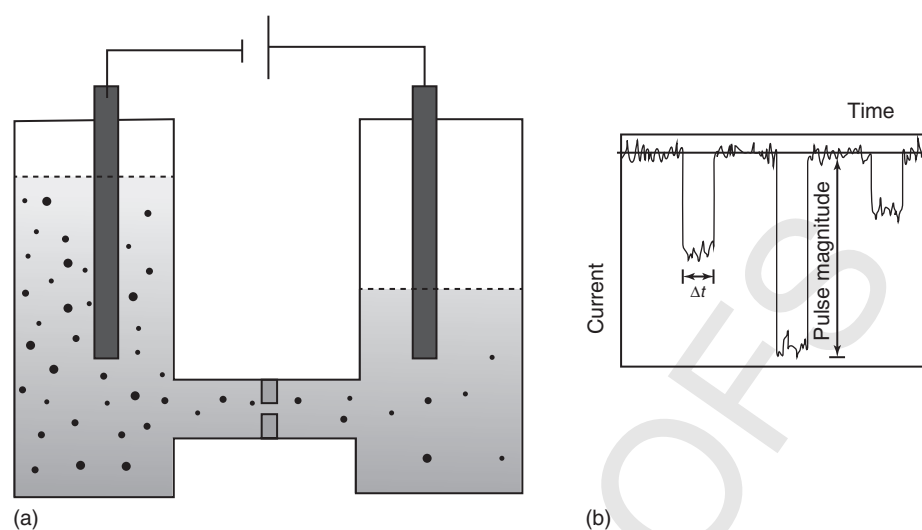
Figure 1 Scheme illustrating the working principle of a Coulter counter: (a) two fluid reservoirs, filled with electrolyte solution, separated by an insulating membrane containing a single channel, under applied electric field; (b) typical current–time recording for particles translocating through a cylindrical channel. The pulse magnitude (height) is proportional to the volume of the analyzed particle. The number of pulses is related with the number of particles flowing through the channel. The pulse duration (width), Δt, indicates the translocation time.

As the detection limit is restricted by the diameter of the sensing channel, the measurement of smaller particles implies the use of smaller pores. In fact, maximum sensitivity is attained in sensing pores with dimensions similar to those of the target particle. In general, the aperture can sense particles with sizes in the range from 2 to 60% (80% in favorable cases) of the aperture diameter.[6] If particles are too small, the change in resistance during particle translocation will be too small to be detected (the magnitude of the voltage pulse is equivalent to the noise level). On the other hand, if particles are larger than the aperture, they cannot translocate. Moreover, broad size ranges can only be covered using multiaperture operations. That requires, however, experienced operators and extra time because larger particles have to be previously removed before using smaller aperture sizes.[5] Commercially available Coulter-based instruments (MULTISIZER™ four from *Beckman Coulter* and ELZONE™ II from *Micromeritics*) have different aperture sizes (up to 2 mm), the minimum aperture diameter of 20 μm is apparently able to sense particles down to 0.4 μm.

It should be emphasized that alternative methods have been applied to size particles in liquid suspensions, namely light scattering techniques that became very popular as they are fast, simple, and cover a wide range of sizes.[7] Regarding nanoparticles, dynamic light scattering (DLS) has been routinely used.[8] In this technique, all particles are measured at the same time, being the size distribution data 'extracted' from a combined signal for all particles (ensemble technique). However, ensemble measurements have typically low resolution and low sensitivity but exhibit broad dynamic ranges (from a few nanometers to a few micrometers), contrary to single particle techniques that normally exhibit high sensitivity but narrow dynamic ranges. DLS is an accurate technique for monomodal distributions (giving an average size value and a polydispersity index) but broad distributions or multimodal samples are frequently not well resolved. In addition, a small amount of very large particles can obscure the contribution of smaller particles.[9–12]

Regarding electrozone sensing, important developments have occurred, mostly in the past two decades, which allow sizing smaller and smaller particles using nanometric apertures. As a matter of fact, the increasing interest in measuring nanoparticles, in addition to advances in micro/nanofabrication and microelectronics, has led to the resurgence of Coulter counters as detectors for a variety of submicron particles such as viruses, pollens, proteins, and DNA molecules, as well as hydrated metal ions, colloids, and natural and synthetic polymers.[13–15] The main reasons why such an 'old' method is once again attracting attention are its simplicity, sensitivity and resolution, and individual single-object measurement.[16–20]

The measurement of nanoparticles naturally requires, as mentioned, nanosized apertures, called *nanopores* or *nanochannels* (a nanopore is a single nanoscale hole with a length-to-diameter ratio about one, whereas a nanochannel has a larger length-to-diameter ratio).

Advances in resistive pulse sensor designs have tremendously improved the minimum detectable size. Furthermore, sensing devices at the nanoscale offer now more information than just particle size and concentration. In fact, as discussed later, information about shape, charge, and conductivity of objects in dispersion can also be ●obtained.[18,21−23]

Q1

DeBlois et al.,[24] in the 1970s, have reported for the first time the extension of the resistive pulse technique to the measurement of submicron particles. They were able to measure polystyrene (PS) beads and viruses <100 nm in diameter, using 500 nm channels fabricated by track etching a polycarbonate (PC) membrane. However, only two decades later, remarkable advances in resistive pulse sensing have been reported, in particular, owing to the advent of new kinds of pores and of ultrasensitive current monitoring equipment. Indeed, this period (1990s) has been regarded as the second revolution in 'hole-based' sensing.[2] In this respect, the works of Bezrukov et al.,[25] who were able to characterize single polymers in solution, and of Kasianowicz et al.[26], who first detected single-polynucleotide molecules (RNA and DNA), represent absolute landmarks. As discussed later, these works sparked a multitude of other works, aiming to develop a method to rapidly and inexpensively sequence genomes using nanopores.[27,28]

Despite the growing interest in pore sensors, they still present some limitations (for example, detection size range, measurement sensitivity, path of the particles through the pore, interactions with pore wall, and time resolution of translocation signals), and improvements in Coulter-based devices are constantly being proposed.[18−20,29−33] In addition, efforts have also been made to integrate these nanopores in microfluidic systems most relevant at the interface between physics, chemistry, and biology.[34−36]

Owing to the explosion of works reported in the literature, especially in the past decade, in a quite dispersed way, it was thought convenient to systematize the latest adaptations of classical Coulter-based apparatus to the measurement of nanoobjects. It should be stressed that a thorough discussion of the electrical sensing zone method applied to micron-sized particles has been published in an earlier paper.[5] The goal of the present survey is to provide a general overview of the existing alternatives to the submicron region with special emphasis on lab-on-chip devices. It has been prepared in a concise manner, aimed more toward nonexperts in the field, and it intends to be a starting point for a more focused research. Despite including many examples related to health sciences (in particular DNA studies, which have catalyzed most of the contemporary studies using resistive pulse sensing), this survey is mainly devoted to the general field of material sciences, namely particle sizing.

It is organized in four sections (besides Introduction): the first one addresses the different kinds of nanopores (biological and synthetic) and reports the recent advances in pore technology; the second one deals with the miniaturization of Coulter counters; the third one reviews the most relevant models of resistive pulse sensing; and the last one includes some final remarks about the technique.

2 BIOLOGICAL AND SYNTHETIC PORES

Various technological developments have been introduced in order to improve nanopore resolution and stability, and different types of pores fabricated with different substrates and technologies have been reported.

Broadly, nanopores can be classified into biological nanopores, which are nanometer-sized protein channels embedded in lipid bilayer membranes; synthetic nanopores, mostly fabricated in thin solid-state membranes (and thus known as 'solid-state nanopores'); and hybrid nanopores, usually biological nanopores embedded in a synthetic membranes.[19,37]

The small dimension of a nanopore permits a nanoparticle or a single molecule to be confined within the nanopore, allowing the extraction of its physical properties. Utilizing the principles of large-scale Coulter counters, if a potential difference is applied across the pore, the translocation of a nanoobject through the pore will result in a transient blockade of the ionic current (or voltage), which can be used to infer information about the sample of interest (Figure 1). Conversely, if information about the translocating particle is known, this data can be used to investigate properties of the pore itself.[38−40]

2.1 Biological Nanopores

Ion channel proteins are naturally occurring nanopores that mediate the flow of ions and molecules across cell membranes.[41] These proteins spontaneously insert into lipid bilayers (either cell membranes or artificial lipid bilayers formed by two monolayers of phospholipids across an aperture in polymer films, as Teflon[42]) and self-assemble to form channels of a few nanometers in diameter.[43]

Major advantages of biological nanopores are their well-defined geometry and structure mapped with atomic precision, great sensitivity, and low noise.[44] Furthermore, they can be genetically engineered and modified by introducing amino acid changes into the genetic material encoding the protein for specific applications as biosensors.[45] Biological nanopores have been broadly used in Nanotechnology and Nanobiotechnology. Current applications include single-molecule mass spectrometry[46]; metal-based nanoparticles
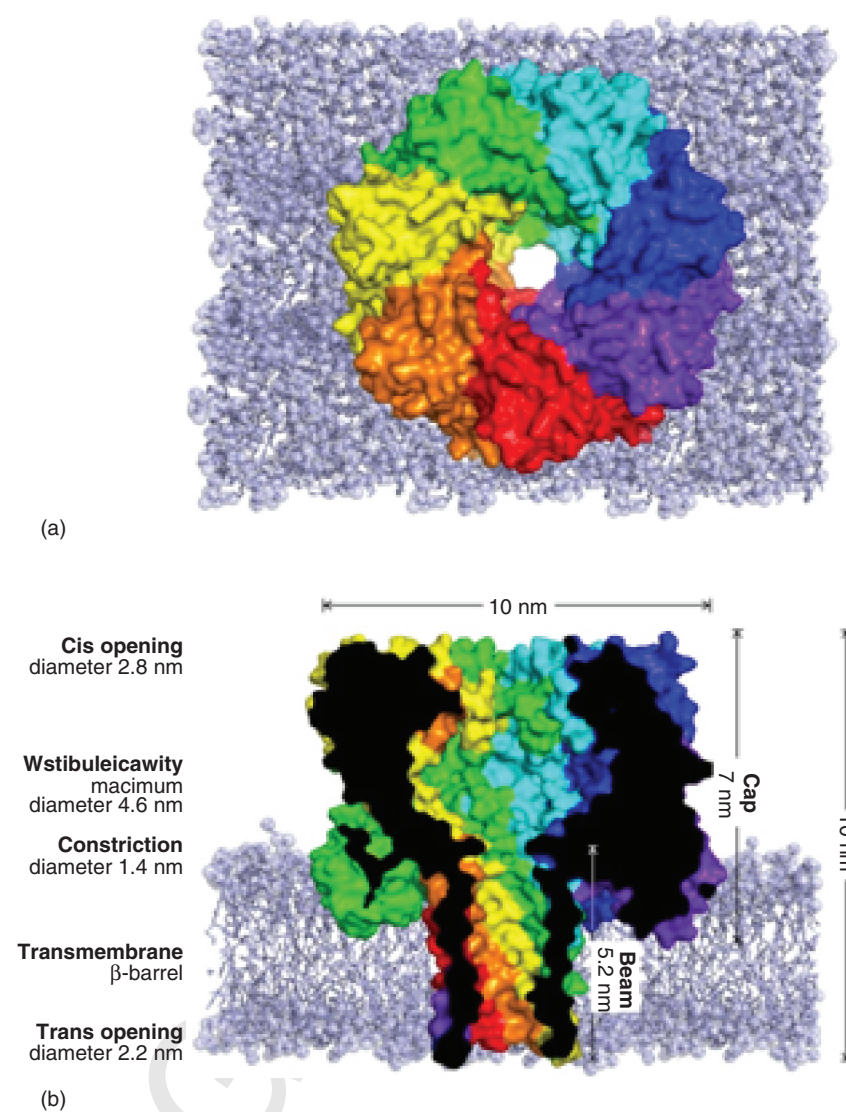
(a)

(b)

Figure 2 Staphylococcal αHL nanopore embedded in a lipid bilayer membrane. (Adapted from Ref. 57.); (a) top view, highlighting each αHL monomer subunit in a different color; (b) cross-sectional view showing the internal diameter of the pore channel at different locations, and the approximate dimensions of the whole complex and of the main domains (rendered from PDB accession code 7AHL[56] using PyMOL software[58]).

characterization[47]; detection of chemical warfare agents,[48,49] explosives,[50] antibiotics,[51] reactive molecules in pharmaceutical products, pesticides, and foodstuffs[52,53]; and, mainly, DNA sequencing.[26,28,54]

Among the commonly applied biological pores in Nano(bio)technology,[55] the most widely used is α-hemolysin[44] (αHL). This 33.2 kDa protein[56] is a toxin secreted by the human pathogen *Staphylococcus aureus* as a monomer. As Figure 2 illustrates, the homoheptameric αHL pore has a mushroom shape with a cap domain and a stem domain connected by the narrowest constriction 1.4 nm in diameter.[56]

Early nanopore studies were performed by Bezrukov and Vodyanoy[59] and collaborators who explored how polyethylene glycols (PEG) partitioned into an ion channel (formed by alamethicin) demonstrating the adequacy of this expedient to molecular scale measurements. Later, PEGs were used to estimate the size of αHL channels. Another important point of these works was to show that ion channels, having functional chemical groups on their interiors, also provide opportunities for chemical interaction between the particles and the pore (typically revealed by changes in the width of resistive pulses).[25,38,59]

Later, in 1996, Kasianowicz et al.[26] were the first to detect single DNA and RNA molecules as they translocated through an αHL nanopore. Because this channel diameter can accommodate only a single strand of RNA and DNA, the channel blockades could be used to measure the polynucleotide length, each base originating a different signal. As mentioned earlier, this study paved the way for numerous works namely the sequential reading of long strands of DNA without chemical modification.[27,28]

Academic nanopore research has been translated into a commercial, electronic-based sensing technology that involves a protein nanopore, in combination with a specific enzyme (*Oxford Nanopore Technologies*). This technology claims to be capable of successful DNA sequencing. The sequencing systems are called 'GridION' and 'MinION', with the GridION representing a high-throughput system and the MinION being a miniaturized system with the size of a USB (universal serial bus) stick.

Although biological pores typically offer great sensitivity and reproducibility, besides low-noise properties, the range of operating conditions and the life time of protein pores and the lipid bilayer membranes in which they are usually assembled are limited (the bilayer often rupture after a few hours of use).[52,61] Another disadvantage is that most biological nanopores have diameters of <2 nm (suitable, for example, for sensing single-stranded DNA but not for double-stranded DNA or larger proteins). Furthermore, they are very sensitive to changes in pH values, temperatures, and transmembrane potentials, which restrict their usage in many engineering devices. Alternative approaches have been developed in order to overcome some of these drawbacks, namely by fabricating artificial nanopores in thin membranes.[44]

2.2 Solid-state Nanopores

In synthetic nanopores, the aperture is formed by the removal of material from an insulating membrane. The dimensions of this aperture are dependent on the method of removal and typically range from single to several hundred nanometers. Most synthetic pores have been fabricated in silicon, silicon nitride, and silicon oxide membranes using different micro and nanotechnologies as, for instance, focused ion beam, various forms of lithography (e.g. electron beam or X-ray lithography), e-beam drilling, or atomic layer deposition.[19,62]

Artificially engineered inorganic membranes offer several advantages over their biological counterparts namely size control, increased chemical and physical (electrical, mechanical, and thermal) stability, besides tunable surface properties, and the ability to be integrated into different micro and nanodevices.[17,19,62] The precise control of nanopore diameters and their inherent high durability have greatly expanded the scope of sensing substrates.[17]

Li et al.[63] were responsible for the first work using a synthetic nanopore, sculpted by focused ion beam and electron beam technologies in silicon nitride. However, it was only in the past few years that artificial nanopores have increased their usefulness, namely after the possibility of being functionally coated in order to mitigate some of their main disadvantages.[64] Actually, the use of silicon-based materials has some drawbacks in electrophoretic applications, in particular their limited wettability, processability, and biocompatibility. Many emerging systems are nowadays fabricated using polymers such as polyimide (PI), PS, PC, polyethylene terephthalate (PET), or polydimethylsiloxane (PDMS).[63,65,66] Recently, a new material has been proposed, poly (methyl methacrylate) (PMMA), a transparent thermoplastic (commonly referred to as acrylics) with several advantages as mechanical and thermal shaping, good electrical resistance, biocompatibility, and long-term stability, which opens the possibility to build the entire detector device with a single material.[62] Compared to the silicon-based materials, polymers are good electrical insulators, which are fairly cheap and can be patterned in a wider selection of processes, namely nanoimprint techniques, particularly interesting for mass production.[67]

Solid-base nanopores can be chemically modified to meet specific requirements. For instance, the binding of polymers to the nanopore is a successful example.[68,69] In particular, temperature-dependent polymers that dehydrate and collapse at high temperatures allow the nanopore diameter to be tuned.[70] Other alternatives use surface charge of the material.[71,72]

Nonetheless, solid-state nanopore technologies also suffer from several practical drawbacks. The major drawback that limits their usefulness for biomolecular studies is that the pore diameter is normally much larger than the distance between two bases in a DNA molecule, which implies that the current blockade is originated not by one but by a large number of bases present in the pore. While the control of nanopore size is possible, it is typically expensive and laborious. Furthermore, synthetic pore sizes cannot be reproduced as precisely as channel proteins and their size and shape, although tunable, can vary from batch to batch.[19] Besides, the ionic current through solid-state nanopores can also suffer from high noise, namely resulting from carbonaceous residues during drilling or adsorption of debris on the nanopore wall.[73] Finally, clogging of the nanopore by analyte molecules can degrade the signal quality, rendering pores unusable for further experiments.[73] Altogether, these effects greatly reduce yield of functional nanopore devices and naturally increase their cost. Solutions to overcome
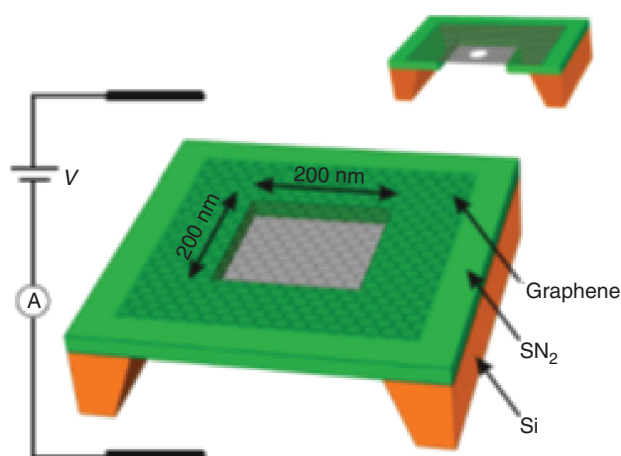
Figure 3 A graphene membrane mounted over an aperture in SiNx suspended across an Si frame. The membrane separates two ionic solutions (not shown) in contact with Ag/AgCl electrodes. Inset, cross section through the Si frame, SiNx aperture, and the graphene membrane through which a nanopore has been drilled. (Reproduced with permission from Ref. 78. © Nature, 2010.)

these aspects have been intensely investigated in the nanopore literature.[74−77]

Alternative substrates have been developed as, for example, graphene membranes and graphene nanopores (Figure 3).[78−81] Graphene membranes exhibit remarkable properties, namely their extremely small thickness [of only one atomic layer (0.3 nm)], most promising for DNA sequencing (DNA moves base by base through the graphene nanopore).[80] The high robust mechanical properties of this material make it quite suitable for nanofluidic systems.[82] In addition, the fact of the graphene being an excellent conductor enables graphene nanopores to be used as a trans-electrode, measuring a current flowing through the nanopore between two chambers.[83−85] Strategies to modify graphene surface in order to improve wetting and to facilitate biomolecule detection and analysis, as well as to develop stable nanopores, have also been reported.[83]

Carbon nanotubes have also been regarded as other alternative synthetic material, as they have well-defined chemical and structural properties, are available in a wide range of diameters (from 1 to 150 nm), and possess uncharged walls that may provide additional information about particle properties.[15,23] In fact, Sun and Crooks[86] (the early 2000s) used a multiwall carbon nanotube-base device (150 nm in diameter) to measure PS particles below 100 nm. This device was later improved to detect simultaneously the size and electrophoretic mobility (surface charge and ζ-potential) of these particles.[21,23] Recently, it was reported the insertion of single-stranded DNA in carbon nanotubes.[87]

Glass nanopipettes have emerged lately as substitutes to biological channels and to nanopores in silicon membranes as they are relatively inexpensive and can be easily prepared.[88−91] Simple devices have been used, which basically require a pipette puller and an amplifier. Quartz is the material of choice to fabricate nanopipettes as it possesses many advantages compared to other type of glasses, in terms of optical transparency, electrical noise, and mechanical properties. The most widely adopted fabrication method for nanopipettes is laser pulling of a glass capillary. The major advantage of the laser pulling method is the simplicity of the approach, as there is no need for expensive equipment, clean rooms, or specialized technicians.[90] Besides, the conical pores are also less susceptible to clogging.[92] These capillaries can then be easily used as classical Coulter counters: the micropipette is filled with KCl solution and immersed in a bath with the same solution, the Ag/AgCl electrodes being placed inside and outside of the capillary. However, the electrochemical behavior of nanopipettes, owing to its conical shape, deviates from that of conventional microelectrodes. For example, conical pores have a smaller resistance and can thus generate higher ion currents for a given voltage.[90,92] This simple resistive pulse platform was found promising to measure and count organic and inorganic nanoparticles.

A new class of artificial pore-based sensors have recently emerged in the market, the so-called tunable resistive pulse sensor (TRPS), also known by the acronym SIOS (scanning ion occlusion spectroscopy).[93,94] In contrast to the pores described earlier, which possess a fixed diameter, limiting the size range of structures that can be effectively analyzed, elastic size-tunable pores allow for further versatility as the pore can be stretched in real time to suit the sample[95] (pore size can be altered by as much as an order of magnitude[96]). However, it should be stressed that other approaches of pore size tuning have been reported in the literature, namely hydrodynamic focusing, described later in the microfluidic section, or using hybrid pores as explained next.

Mechanically, active pore-based analyzers have been commercialized by *IZON Science Ltd.*, as *qNano*,[97] covering a range of particle diameters between 50 nm and 10 μm (being typically used to measure particles with one dimension larger than 100 nm). This device is portable and seems a good alternative for quality control in particle analyses. The tunable pore is fabricated by puncturing an elastic polyurethane 'cruciform' membrane, producing a cone-shaped elastic pore, mounted on adjustable jaws, as shown in Figure 4. The four arms of the cruciform can be mechanically stretched and/or relaxed in the *XY*-axis. The pore size is tuned to the particle sample in real time by adjusting the axial strain applied to the membrane. This has been used by various research groups to measure
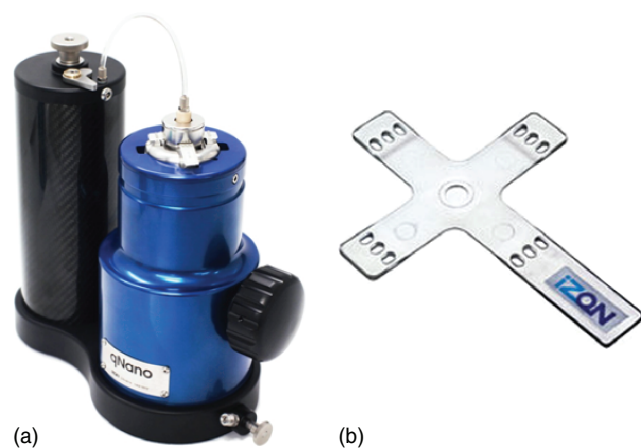
(a)   (b)

Figure 4 Photograph of (a) the commercially available tunable resistive pulse sensors (TRPS) – Izon qNano system – and of (b) the elastic nanopore membrane located at the inner septum ring at the center of the cruciform.[97] (Reproduced with permission of Izon, Ltd.)

Figure 5 DNA origami schematic. (Reproduced with permission from Ref. 103. © John Wiley & Sons, Ltd, 2012.)

size, shape, number concentration, and surface charge of synthetic and biological particles.[18,94,98]

2.3 Hybrid Approaches

The concept of hybrid pores was firstly demonstrated by Hall.[99] in 2010, by inserting a single, preassembled αHL protein pore into a thin SiN membrane. This strategy aimed to combine the selectivity and sensitivity of biological pores with the mechanical stability of an inorganic scaffold. However, the blockade amplitudes detected were significantly low and an increase in electrical noise was observed. Although these parameters had to be optimized, this hybrid architecture opened an avenue of new possibilities in this field. Conversely, synthetic structures such as ultrashort single-walled carbon nanotubes[100] can be integrated into a lipid layer to investigate DNA translocation. Nanotubes (single-walled nanotubes) have also being complexed with DNA and protein for resistive pulse sensing.[101] Other examples reported in the literature include coating synthetic nanopores with organic molecules[64,102] or, more recently, fluid coatings, creating lipid bilayer-coated pores.[29,85] Fluid coating enables not only the tailoring of surface chemistry but also the dynamic variation of pore diameter in small increments. Moreover, incorporating ligands in the fluid bilayer was found to slow the translocation of target proteins, enabling the extraction of more valuable information.[29]

Moreover, in the past couple of years, the capabilities of DNA as a nanoscale building material have also been explored and many structures have been constructed utilizing the scaffold origami method[31−33,36,103,104]
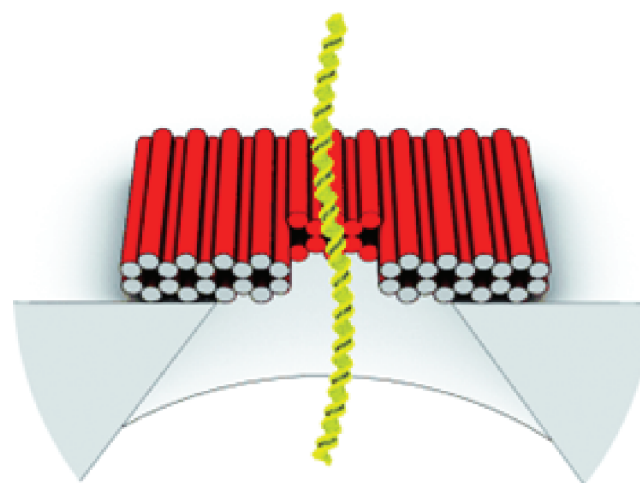
(Figure 5). The combination of DNA origami structures with solid-state nanopores[103,105] or embedded in fluid bilayers[31,104] constitutes a novel approach for the formation of hybrid nanopores. DNA origami structures have also been trapped in glass nanocapillaries.[33] These original strategies offer the possibility of programmable nanopores with tunable size and geometry. Moreover, it opens the possibility of utilizing these hybrid structures as smart nanopores whose behavior can be controlled by external stimulus.[33]

Finally, it should be stressed that the development of nanopores is still underway and the number of alternatives/possibilities in nanopore sensing will continue to grow rapidly.

3 MICROFLUIDIC DEVICES

Advances in microfabrication resulted in increasingly sophisticated microfluidic systems that led to true 'lab-on-chip' devices. These can integrate conduits that approach molecular length. The incorporation of biological and synthetic nanopores in fluidic devices holds great promise for new analytical applications as biomedical research, environmental monitoring, food monitoring, and drug screening. Many miniaturized versions of the Coulter counter have been reported to detect and quantify micro- and nanoscale particle-like structures, including pollens, bacteria, viruses, and biomolecules. The main advantages of these devices are portability, compactness, reduced cost and reagent consumption, high throughput, and the ability to integrate multiple functions. Some lab-on-chip devices are simply scaled down versions of conventional techniques; others are equipped with novel functions

taking advantage of the small length scales and laminar flow characteristics in microsystems.[13,106,107]

The first Coulter counter microchip was reported by Larsen[108]. This device, fabricated on a silicon substrate, was similar to a conventional Coulter counter but was modified to adapt the principle into a planar microchannel system, employing hydrodynamic focusing (explained next) to reduce particle clogging in the sensing channel. Later, Koch et al.[109] (1999) and Roberts et al.[110] designed similar devices. A special mention is due to the work of Saleh and Sohn,[111] in the early 2000s, who designed a microchip Coulter counter on a quartz substrate to discriminate colloids as small as 87 nm, being able to discriminate particles whose diameters differed by <10%.[112] Later, they developed a PDMS-based device that not only detected single molecules but was able to detect the binding of unlabeled antibodies to the surface of latex colloids.[113,114] They have also described how off-axis particles affect the data and have developed an algorithm to remove those effects.[115] Figure 6 shows representative data of monodisperse and polydisperse solutions containing colloids analyzed with these microdevices.[112]

Multiple designs of micro fluidic devices have been proposed by various researchers.[14,109,116−118] Despite
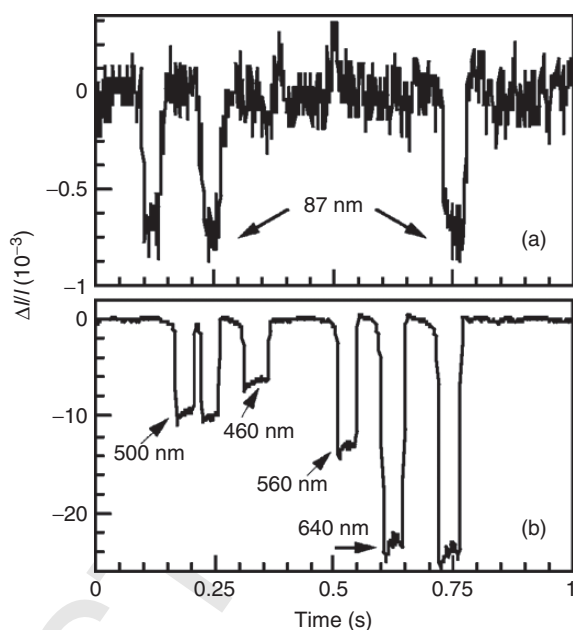
Figure 6 Measurements of normalized current ($\Delta I/I$) versus time for (a) a monodisperse solution of 87 nm latex colloid, and (b) a polydisperse solution of latex colloids with diameters 460, 500, 560, and 640 nm, showing clear differences in the pulse heights caused by particles of different sizes. (Reproduced with permission from Ref. 112. © American Institute of Physics, 2001.)

the efforts to implement these microdevices, most still presented some limitations, namely the possibility of using the same device to cover a broad range of particle sizes or to achieve high throughputs. Attempts to overcome these limitations have been proposed by several researchers, as discussed in the following sections.

3.1 Hydrodynamic Focusing

Most of the apparatuses implemented possess apertures with sizes comparable to the size of the particles of interest in order to increase accuracy/sensitivity, hence not allowing the use of the same aperture with broad size ranges. One expedient that has been adopted to overcome this is is to use hydrodynamic focusing to confine the particle stream to a smaller cross section, thus being able to detect particles with a broad range of sizes using the same device. This is normally achieved by two sheathed fluid streams (of a nonconductive fluid) placed on each side of the sample fluid, as illustrated in Figure 7. This approach has two purposes: to focus the sample fluid into a single stream moving along the central axis of the pore, avoiding distorted pulses (which result in incorrect particle information), and to adjust the sample stream dimensions (expanding or compressing, simply by adjusting the sheath and sample flow rate ratios, i.e. without the need to exchange any parts), allowing the active area of the device to be effectively confined to the size of the focalized stream, thus improving measurement resolution and sensitivity. In addition, hydrodynamic focusing also minimizes channel clogging risk.[118] Originally, only 1-D systems were used, although other fabrication schemes have been proposed to achieve 2-D approaches focusing.[119,120] More recently, 3-D hydrodynamic focusing techniques (with more elaborated fluid cells) have been reported, which result in 2.5 times increase in signal strength over devices that only focus the
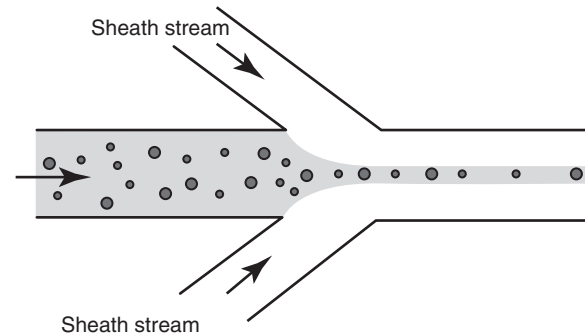
Figure 7 Schematic of standard hydrodynamic focusing that consists of squeezing the sample flow by additional side streams, confining it to a limited portion of the sensing channel.
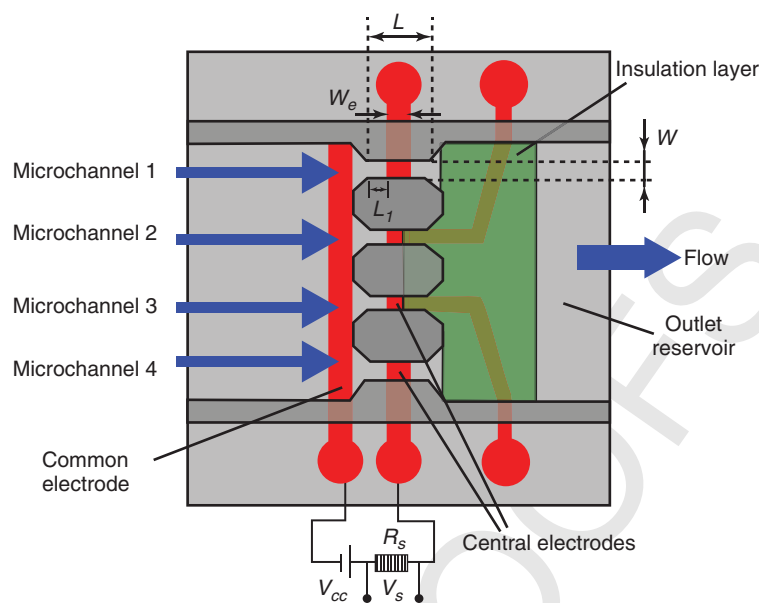
Figure 8 Schematic of the on-chip multichannel Coulter counter-based device, showing four parallel sensing microchannels, connected by four sensing electrodes located in the center of the microchannels. (Reproduced with permission from Ref. 14. © IOP Publishing, 2007.)

sample in the horizontal direction.[118,121,122] Nonetheless, this approach has still been questioned.[18,123]

3.2 Multiple Pores

Another limitation that has been mentioned in microfluidic devices is the limited throughput achieved when using single pores. In fact, in these devices, only very small volumes of sample can be processed at a time (the flow rate is proportional to the pore cross section). In addition, the particles are generally present in very low concentrations. Thus, analyzing bulk volumes would take too much time.[13]

The throughput can be improved by increasing the particle velocity using a large pressure gradient. However, if particles move faster, their translocation time in the pore will be shorter originating a loss of information, because of the sharp shape of the measurement pulses. These pulses would require sophisticated hardware and signal processing, nonpractical for portable systems.[14]

Higher throughputs can alternatively be achieved using a device with multiple channels operating in parallel. In this way, the flow volume rate is increased by the number of channels, whereas the fluid flow velocity could be kept low, thus reducing testing time and improving system efficiency.

Carbonaro and Sohn,[124] in 2005, integrated two pores on a single on-chip Coulter counter to perform multianalyte immunoassay detection. More recently, devices with a single reservoir and four parallel microchannels, each equipped with individual detection, have been fabricated ~~by Jagtiani et al.~~[14,125] The microchannels and reservoirs were built in PDMS using soft lithography technologies and bonded to a glass substrate (Figure 8). The device has a common electrode placed in the inlet of the reservoir at the entrance of the microchannels and four central electrodes at the center of each microchannel. The central electrode divides each microchannel into two equivalent half microchannels: the first half is used as the sensing channel (counting particles passing by), whereas the second half is used as an isolating resistor to reduce the cross-talk among channels. The voltage pulses across each sampling resistor can be recorded and analyzed separately. In contrast to a single-channel Coulter counter, the sensor can detect particles through its four sensing channels simultaneously. The original device has been improved to include multiplex detection requiring only a single set of detection electronics. Tests using $30 \, \mu m$ PS particles showed an improvement of 300% in throughput over a single-channel device, without compromising the sensitivity and reliability of a single-channel measurement.[13] According to the authors, the multiplex detection system can be expanded to a larger number of channels. Figure 9 illustrates the actual size of microfabricated device.
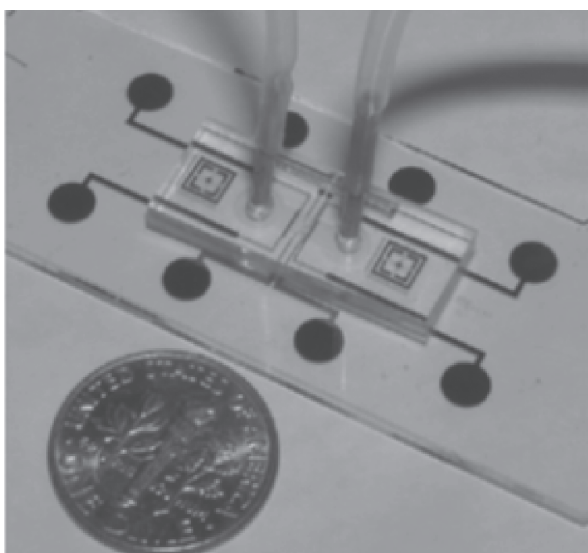
Figure 9 Picture of the microfabricated device (with fluidic connections) together with a one dime coin (17.9 mm in diameter). (Reproduced with permission from Ref. 13. © IOP Publishing, 2011.)

3.3 Signal-to-noise Ratio

An alternative approach to improve measurement sensitivity without dramatically decreasing the volume of the sensing channel is to use instrument amplifications and noise reduction from fluid circuit and electronic sensing system. In this way, it is possible to detect small particles inside microscale apertures that can be easily fabricated using soft lithography.[124,126] Sridhar et al.[67] have reported a design of fluidic sensors that integrates a fluidic circuit with metal-oxide-semiconductor field effect transistor (MOSFET). In this circuit, particles are detected by monitoring the MOSFET drain current instead of the ionic current through the fluidic circuit as in traditional resistive pulse sensors. This can increase the sensitivity by amplifying the percentage of the modulation caused by the translocation of the particles through the sensing channel, resulting in a decrease in the volume ratio between the particle and sensing channel (10 times smaller than the lowest ratio reported in the literature for commercial Coulter counters).[67,127] In addition, this system was able to distinguish two similarly sized microbeads with different surface charges (4.84-µm diameter polystyrene and 4.8-µm diameter glass microbeads).

3.4 Particle Sorting

Finally, besides counting and sizing, a number of groups have developed prototype microchip-based flow cytometers that are able to sorting particles, based on their size.

Continuously sorting particles or cells from a heterogeneous suspension is of critical importance in many applications such as combinatorial chemistry, clinical diagnostics, water and food quality monitoring, and biohazard detection.[35,128] Lab-on-a-chip devices have been developed that combine sorting methods in feedback with high-sensitivity microfluidic volume sensors. Various kinds of microfluidic sorting mechanisms such as electrokinetics, hydrodynamics, and hydrophoresis have been used.[128] For instance, Song et al.[35] reported a sorting device where cells were sorted one at a time by electrokinetic flow manipulation. A single-gate differential resistive pulse sensor is employed to electrically detect the sizes of particles driven by electroosmotic flow. Whenever the target particles were detected, the resistive pulse signals would activate the sorting process by applying a DC pulse voltage and the target particle would be electroosmotically sorted to the adequate collecting channel. This method was applied to automatically detect and sort PS particles and microalgae in aqueous solutions, sorting 5 µm particles from a mixture of 4 and 5 µm particles.

More recently, Riordon et al.[129] used a hydrodynamic flow sorting system, where output into one of several collection ports is achieved through pressure-driven flow focusing and redirection as illustrated in Figure 10. With this system, 5.6 µm PS microspheres were extracted from a solution that also contained 8.3 µm and 3.9 µm particles with very high efficiencies (close to 97.3%).

4 ELECTRICAL SIGNATURE OF PARTICLE TRANSLOCATIONS

As mentioned earlier, the presence of a nonconducting particle in a pore increases its resistance, leading to a series of resistance 'pulses' (or blockade events) that can be generally described by their magnitude (pulse height), proportional to the excluded volume of the particle, frequency, related to the particle velocity, and duration (pulse width), which indicates the translocation time of the particle though the pore. These pulses are dependent on both particle and pore properties and, for cylindrical pores and spherical particles, are typically square signals as illustrated in Figure 1.

From the frequency, magnitude, duration, and shape of the generated pulses, information about size, shape, concentration, and charge can, in adequate conditions, be derived. To extract this information, it is necessary to use theoretical models, in addition to knowing the pore dimensions and the measurement conditions. Although the discussion of these models is out of the scope of this survey, a brief analysis of the strategies currently adopted to extract information from the current blockades is given.
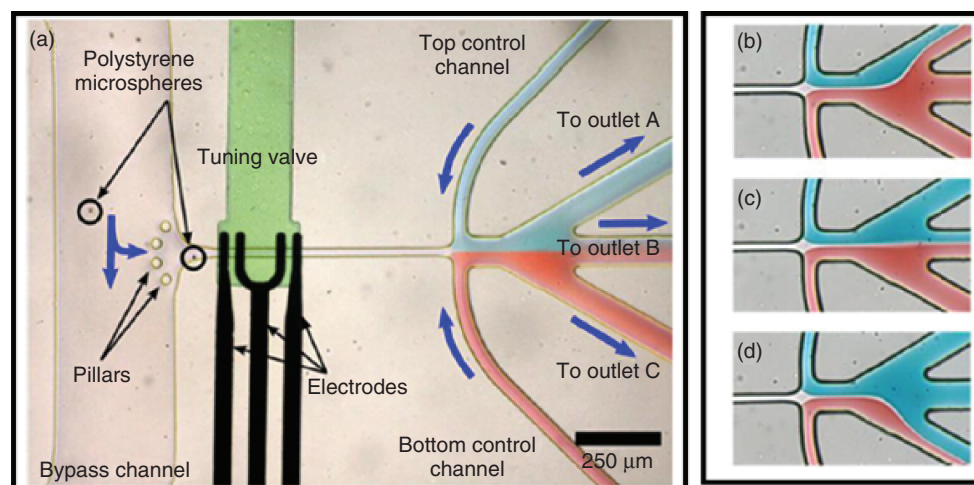
Figure 10 (a) Resistive pulse sensor with pressure-based flow sorting. A tuning valve is used to adjust the height of the sensing channel above the electrodes. Pillars fence the channel entrance, preventing agglomerations of particles from obstructing the sensor. Microspheres are pressure-driven through the sensor where pulse amplitude is acquired. The signal is then analyzed by devoted software, which automatically redirects the central flow stream into one of the three outlets (b–d). Blue arrows denote flow direction.[129] (Adapted by permission of Elsevier.)

The height of the measured pulses depends on the fraction of the volume of the sensing channel that is occluded by the particle being sensed. In 1970, DeBlois and Bean[24] derived an expression for the change in the resistance of a cylindrical sensing channel (with a diameter D and a geometrical length L) in the presence of a spherical, insulating particle (of diameter d). By solving Laplace's equation with spherical boundary conditions, they showed that the increase in resistance of the cylindrical sensing channel, ΔR, owing to the presence of the spherical particle can be written as

$$\Delta R \approx \frac{4\rho_{fluid}d^3}{\pi D^4} \tag{1}$$

where ρ_{fluid} represents the resistivity of the conducting electrolyte. However, Equation (1) is only valid when $d/D \ll 1$ and $D/L < 1$. In these conditions, the relative resistance modulation is given by

$$\frac{\Delta R}{R} = \frac{d^3}{D^2 L} = \frac{3}{2}\frac{V_p}{V_c} \tag{2}$$

where V_p and V_c are the volumes of the spherical particle and sensing channel, respectively, and R the pore resistance (without particles). (When L is comparable to D, the geometrical length should be substituted by the effective resistive length $L_R = L + 0.8\,D$, where the factor $0.8\,D$ corrects for the so-called 'end effect', which becomes significant for thin pores.) This expression clearly shows that the relative resistance modulation is roughly equal to the volume ratio of the particle to the sensing channel.

Thus, altering the pore size will change the measurement sensitivity (in other words, using smaller pores enables better sensing smaller particles). In addition, as pulse signal is proportional to the diameter cubed, very small differences in particle size results in large differences in the pulse heights.

When a constant voltage is applied across the sensing channel, and considering the particle much smaller than the channel, it comes from Ohm's law:

$$\frac{\Delta I}{I} \approx \frac{\Delta R}{R} \tag{3}$$

Therefore, the relative ionic current modulation, $\Delta I/I$, will also be roughly equal to the volume ratio of the particle with respect to the channel, V_p/V_c. Similarly, if the ionic current is kept constant, then a corresponding voltage modulation will occur.

However, when the particle size becomes comparable to that of the channel, higher order correction terms will become important and the relationship between the volume ratio of the particle to the channel and the relative resistance modulation will take a more complex form. In fact, a variety of models have been proposed in the literature to estimate the resistance variance exerted by a single particle translocating through a pore. None of them, however, is valid for all kinds of pores in terms of various shapes and dimensions. A general equation, often adopted, is[24,130]

$$\frac{\Delta R}{R} = f\frac{V_p}{V_c}S\left(\frac{d}{D}\right) \tag{4}$$

This equation considers the effect of particle shape through a shape factor f, and it is also dependent on particle orientation inside the pore ($=2/3$ for spherical particles)[18] and the nonideal effects of electrical field line 'bulging' due to the particle-to-pore size ratio (d/D) via a size factor S (these effects are resultant of the fact that a potential difference across the pore creates tubular current streamlines inside the cylindrical pore that slightly bulge around the translocating sphere).[24] An empirical correlation commonly used for S is

$$S\left(\frac{d}{D}\right) = \left[1 - 0.8\left(\frac{d}{D}\right)^3\right]^{-1} \quad (5)$$

In addition to particle size, particle concentration can also be extracted from pulse signals. In fact, the frequency of the pulses, J (number of events per unit time), can be correlated to particle concentration, C, as[130]

$$C = \frac{J}{Q} \quad (6)$$

where Q is the fluid flow rate. This expression is valid if electrophoretic velocities are small compared to fluid velocities and also neglects electroosmosis effects (as discussed later). In these conditions, Q can be calculated using Hagen–Poiseuille equation as

$$Q = \frac{\pi P D^4}{128 L_H \eta} \quad (7)$$

where P is the pressure difference across the pore, η the viscosity of the fluid, and L_H the effective hydrodynamic length of the pore ($=L + 0.6 D$)[130]

Substituting Q in Equation (6) leads to

$$C = \frac{128\,\eta\,L_H}{\pi\,D^4}\,K \quad (8)$$

where K ($=J/Q$) can be derived from the slope of a plot of particle frequency versus pressure. This expression can be used to calculate particle concentrations using two different methods: from the slope K, knowing all the other variables, or using a calibration sample of known concentration.[15,131]

Finally, the other measurable parameter of the resistive pulses is their duration (pulse width), (Δt), that can, in some cases, be used to calculate the electrophoretic mobility of the particles and hence their electrokinetic surface charge. Δt is related to the transport velocity of the particle (v_s), which in turn is determined by the transport properties of the particle as it transverses the pore. It should be pointed out that transport in nanoporous media differs significantly from

ordinary transport in bulk media, mainly because the interactions between a pore surface and the nanoparticle being transported become increasingly important as the dimensions of the pore approach the size of the particle.

In the absence of specific chemical interactions between the particles and the pore itself, there are four fundamental transport mechanisms that can potentially contribute to particle velocity (v): pressure-driven flow (v_{PD}), electrophoresis (v_{EP}), electroosmosis (v_{EO}), and diffusion (v_D), as expressed by Equation (9)

$$v_s = v_{s,\,PD} + v_{s,\,EP} + v_{s,\,EO} + v_{s,\,D} = \frac{D^2}{32\eta l_R}\Delta P$$
$$+ \frac{\mu}{L_R}E_M + \frac{\varepsilon\xi_c}{4\pi\eta L_R}E_M + \frac{\mathcal{D}}{L_R C}\Delta C \quad (9)$$

In this equation, η is the solution viscosity, ΔP the pressure across the channel, μ the electrophoretic mobility of the particle, ε the solution dielectric constant, ζ_c the ζ-potential of the channel surface, E_M the membrane potential, $\mathcal{D}$ the diffusion coefficient of the particle, C the particle concentration in the chamber containing the source solution, ΔC the difference between the particle concentrations in the source and receiving solutions, and L_R effective resistive length ($L_R = L + 0.8\,D$).

However, when all four transport modes are operative, it is difficult to extract useful analytical information, because the transport modes are interdependent and, therefore, the equations governing particle velocity are complex.[15,18,22] The situation is simplified only when a single mode of transport dominates the other three. Furthermore, although present, Brownian motion (e.g. diffusion) is typically considered to be negligible within the pore and thus only the other three terms need to be considered.[15,18,86]

Thus, for instance, if the electrophoresis is the dominant transport mode (valid for charge neutral channels, as carbon nanopores[21]), transport time can be directly related to electrophoretic mobility μ, defined as average particle speed per unit field gradient by Equation (10)[21]

$$\mu = \left(\frac{L + 0.8D}{\Delta t}\right)\left(\frac{E_M}{L + 0.8D}\right)^{-1} = \frac{(L + 0.8D)^2}{E_M \Delta t} \quad (10)$$

In addition, the electrophoretic mobility is linked to the surface charge Q, according to[21]

$$\mu = \frac{Q}{2\pi\eta d\left(1 + \frac{d}{2d_D}\right)} \quad (11)$$

where η is the viscosity of the solution, d the particle diameter, and d_D the Debye length. It should be noted that the above equation is derived by combining the Helmholtz–Smoluchowski equation and the Debye–Hückel approximation; thus, it is applicable only to the case where the particle size is much larger than the electrical double layer and the surface potential ζ is small.[21]

Combining Equations (10) and (11) leads to

$$Q = \frac{2\pi\eta(L + 0.8D)^2 d\left(1 + \frac{d}{2d_D}\right)}{E_M \Delta t} \qquad (12)$$

This equation shows that, when transport through a cylindrical channel is dominated by electrophoresis, the surface charge of each individual particle can be calculated merely from pulse characteristics: pulse height [that allows the calculation of size (d)] and pulse width (Δt).

Other examples that have been used to elucidate colloidal dispersions can be found in the literature.[22,30] Such studies are most relevant not only in nanoscale colloids but, in general, to investigate mass transport phenomena in nanoporous media.

5 FINAL REMARKS

The need for sizing techniques that enable fast, easy, and accurate analysis of nanoparticles in solution is determinant not only because the knowledge of particle size is crucial to understand their behavior but also because many other particle characteristics are quantified as a function of size. Thus, the emergence of techniques for this size range, capable of providing reliable sizes and additional particle information, preferably in an individual basis, is obviously of great interest.

As the electrical sensing zone method is a well-established technique for micron-sized particles, its strongest points being its sensitivity and simplicity, and especially the fact of being a single particle technique, its adaptation to the nanoscale measurement is certainly regarded with much interest (and naturally some caution). The fact that this technique is independent of the particles optical properties and well correlated with particle volume is also regarded as a major advantage. As mentioned earlier, nanopore-based resistive pulse measurements have been applied to sensing and analyzing many submicron particles, including viruses, synthetic particles, and biomolecules, being able to discriminate between particles of different functionalization.[47,113] As noted in the Section 1, DLS has been intensely used for this particle range owing to its applicability to a wide range of sizes and dispersion media and for not requiring calibration.[132] It is noteworthy that calibration of nanoscale resistive sensors, as in classical Coulter-based devices, is performed using a particle suspension of a known size as a reference (the particle size distribution of the unknown sample is calculated using a comparison between the blockade magnitude distributions of the calibration and unknown samples[95]). However, DLS has also been subject to some criticisms mainly related to its limitation to resolve multimodal distributions and for being shape dependent (especially extreme shapes, as rod-like particles) and affected by the presence of large particles, even if in small amounts.[11,12] Besides, the conversion of intensity-based distributions to volume and number distributions requires information on particle refractive index, not always available.

Recently, especially after the commercialization of tunable resistive pulse sensing (TRPS) devices (as *qNano*, from *IZON Science Ltd.*[97]), many comparative studies have been undertaken with benchtop techniques, namely TRPS and DLS.[132−134] In general, resistive pulse sensing presents some advantages regarding resolution (as expected from a counting technique)[133] and sensitivity (being able to work with lower concentrations than DLS)[132]. Nonetheless, DLS exhibits a much wider size range than the tunable resistive pore sensing.[134] Moreover, when using pore stretching facilities (and like in the classical Coulter devices), some difficulties have been found to integrate the measurements carried out with different pore sizes under varying experimental conditions[132,133] (it should be pointed out that tunable pores require calibration at each stretch). Regarding accuracy, results with tunable pores have shown good agreement (within 6%) with TEM for a range of monodisperse samples.[95] Curiously, comparisons with conventional Coulter-based devices, for the micron-sized range, have not been reported. An overall conclusion is, however, that measuring by more than one method is highly recommended as different techniques provide different and complementary particle information.[133−135]

Finally, it should be highlighted that most of the works reported in the literature with resistive pulse sensors are related with research studies to investigate the potentialities of this technique, namely in DNA sequencing. Although many involve model systems (i.e. spherical particles, mainly PS particles, including carboxylated particles), rod-shaped particles have also been studied with tunable nanopores.[98] On the other hand, most of the devices employed were built for specific purposes (homemade Coulter counters) and thus a wide variety of experimental setups have been reported. In fact, from the aforementioned cited works, it can be concluded that different types of nanopores

(from biological to solid state), with distinct dimensions (from one to several hundred nanometers), made of different materials (silicon, PC, glass, PDMS, graphene, and carbon nanotubes) have been used. In addition, quite different experimental conditions have been adopted. For instance, electrical detection of the particles has been performed by either direct or alternating current measurements; different voltages have also been applied (typically <1 V, and more frequently <0.1 V), as well as current pulses of different amplitude (typically in the order of nanoampere), which in turn have been optimized through manipulations of voltage, particle or electrolyte concentration, pressure or by tuning the pore size. Regarding electrolytes, solutions such as NaCl (1 or 0.1 M) and KCl (0.1 M), with distinct wetting agents (to reduce adhesion to the pore walls), have been used. On the other hand, it has also been mentioned that previous sample filtering is needed in order to prevent pore blockage (e.g. using filters with pores of similar size as the pore size[121,131,136,137]), or that measures have to be ~~been~~ taken to minimize particle aggregation (as for example, pipetting,[113] reversing voltage,[47,138] applying high electric field pulses,[73] or exploiting the tunability of the pores[131]).

All these aspects have to be addressed in a consistent manner for this technique to be accepted as a recognized and widespread technique, such as the conventional Coulter method that has been adopted as a standard method by several international institutions for standardization.[5] Indeed, detailed protocols, standardized procedures, and interlaboratory tests with standard materials are needed before resistive pulse sensing be adopted as an alternative and/or complementary method to those routinely used for sizing particles at the nanoscale.

ABBREVIATIONS AND ACRONYMS

DLS	Dynamic Light Scattering
MOSFET	Metal-Oxide-Semiconductor Field Effect Transistor
PC	Polycarbonate
PDMS	Polydimethylsiloxane
PEG	Polyethylene Glycols
PET	Polyethylene Terephthalate
PI	Polyimide
PMMA	Poly (Methyl Methacrylate)
PS	Polystyrene
SIOS	Scanning Ion Occlusion Spectroscopy
TRPS	Tunable Resistive Pulse Sensing
TRPS	Tunable Resistive Pulse Sensor
USB	Universal Serial Bus

REFERENCES

1. W.H. Coulter, Means for Counting Particles Suspended in a Fluid, *US Patent 2656508*, 1953.

2. M. Wanunu, 'Nanopores: A Journey Towards DNA Sequencing', *Phys. Life Rev.*, **9**, 125–158 (2012).

3. T. Allen, *Particle Size Measurement: Volume 1: Powder Sampling and Particle Size Measurement*, Springer, Netherlands, 1996.

4. H.G. Merkus, '*Electrical Sensing Zone*', in *Particle Size Measurements*, Springer, Netherlands, 241–257, 2009.

5. M.M. Figueiredo, '*Electrozone Sensing in Particle Size Analysis*', in *Encyclopedia of Analytical Chemistry*, John Wiley & Sons, Inc., New York, 2006.

6. J.G. Harfield, R.T. Wharton, R.W. Lines, 'Response of the Coulter Counter® Model ZM to Spheres', *Part. Part. Syst. Charact.*, **1**, 32–36 (1984).

7. H.G. Merkus, *Particle Size Measurements - Fundamentals, Practice, Quality*, Springer, Netherlands, 2009.

8. B.J. Berne, R. Pecora, *Dynamic Light Scattering: With Applications to Chemistry, Biology, and Physics*, Courier Dover Publications, New York, 2000.

9. R. Finsy, 'Particle Sizing by Quasi-Elastic Light Scattering', *Adv. Colloid Interface Sci.*, **52**, 79–143 (1994).

10. H. Ruf, B.J. Gould, W. Haase, 'The Effect of Nonrandom Errors on the Results from Regularized Inversions of Dynamic Light Scattering Data', *Langmuir*, **16**, 471–480 (1999).

11. Å.K. Jamting, J. Cullen, V.A. Coleman, M. Lawn, J. Herrmann, J. Miles, M.J. Ford, 'Systematic Study of Bimodal Suspensions of Latex Nanoparticles using Dynamic Light Scattering', *Adv. Powder Technol.*, **22**, 290–293 (2011).

12. H. Kato, A. Nakamura, K. Takahashi, S. Kinugasa, 'Accurate Size and Size-Distribution Determination of Polystyrene Latex Nanoparticles in Aqueous Medium Using Dynamic Light Scattering and Asymmetrical Flow Field Flow Fractionation with Multi-Angle Light Scattering', *Nanomaterials*, **2**, 15–30 (2012).

13. A.V. Jagtiani, J. Carletta, J. Zhe, 'A Microfluidic Multichannel Resistive Pulse Sensor Using Frequency Division Multiplexing for High Throughput Counting of Microparticles', *J. Micromech. Microeng.*, **21**, 065004 (2011).

14. A.J.J. Zhe, P. Dutta, J. Hu, J. Carletta, 'A Micromachined High Throughput Coulter Counter for Bioparticle Detection and Counting', *J. Micromech. Microeng.*, **17**, 304–313 (2007).

15. R.R. Henriquez, T. Ito, L. Sun, R.M. Crooks, 'The Resurgence of Coulter Counting for Analyzing Nanoscale Objects', *Analyst*, **129**, 478–482 (2004).

16. H. Bayley, C.R. Martin, 'Resistive-Pulse Sensing From Microbes to Molecules', *Chem. Rev.*, **100**, 2575–2594 (2000).

17. C. Dekker, 'Solid-State Nanopores', *Nat. Nanotechnol.*, **2**, 209–215 (2007).

18. D. Kozak, W. Anderson, R. Vogel, M. Trau, 'Advances in Resistive Pulse Sensors: Devices Bridging the Void Between Molecular and Microscopic Detection', *Nano Today*, **6**, 531–545 (2011).

19. F. Haque, J. Li, H.-C. Wu, X.-J. Liang, P. Guo, 'Solid-State and Biological Nanopore for Real-Time Sensing of Single Chemical and Sequencing of DNA', *Nano Today*, **8**, 56–74 (2013).

20. I.Y. Wong, S.N. Bhatia, M. Toner, 'Nanotechnology: Emerging Tools for Biology and Medicine', *Gens Dev.*, **27**, 2397–2408 (2013).

21. T. Ito, L. Sun, R.M. Crooks, 'Simultaneous Determination of the Size and Surface Charge of Individual Nanoparticles Using a Carbon Nanotube-Based Coulter Counter', *Anal. Chem.*, **75**, 2399–2406 (2003).

22. G.R. Willmott, R. Vogel, S.S.C. Yu, L.G. Groenewegen, G.S. Roberts, D. Kozak, W. Anderson, M. Trau, 'Use of Tunable Nanopore Blockade Rates to Investigate Colloidal Dispersions', *J. Phys. Condens. Matter*, **22**, 454116 (2010).

23. T. Ito, L. Sun, R.R. Henriquez, R.M. Crooks, 'A Carbon Nanotube-Based Coulter Nanoparticle Counter', *Acc. Chem. Res.*, **37**, 937–945 (2004).

24. R.W. DeBlois, C.P. Bean, 'Counting and Sizing of Submicron Particles by the Resistive Pulse Technique', *Rev. Sci. Instrum.*, **41**, 909–916 (1970).

25. S.M. Bezrukov, I. Vodyanoy, V.A. Parsegian, 'Counting Polymers Moving Through a Single Ion Channel', *Nature*, **370**, 279–281 (1994).

26. J.J. Kasianowicz, E. Brandin, D. Branton, D.W. Deamer, 'Characterization of Individual Polynucleotide Molecules Using a Membrane Channel', *Proc. Natl. Acad. Sci. U.S.A.*, **93**, 13770–13773 (1996).

27. J. Rosenstein, 'The Promise of Nanopore Technology: Nanopore DNA Sequencing Represents a Fundamental Change in the Way that Genomic Information is Read, with Potentially Big Savings', *IEEE Pulse*, **5**, 52–54 (2014).

28. S. McGinn, I.G. Gut, 'DNA sequencing – Spanning the Generations', *N. Biotechnol.*, **30**, 366–372 (2013).

29. E.C. Yusko, J.M. Johnson, S. Majd, P. Prangkio, R.C. Rollings, J. Li, J. Yang, M. Mayer, 'Controlling Protein Translocation through Nanopores with Bio-Inspired Fluid Walls', *Nat. Nanotechnol.*, **6**, 253–260 (2011).

30. D. Kozak, W. Anderson, R. Vogel, S. Chen, F. Antaw, M. Trau, 'Simultaneous Size and ζ-Potential Measurements of Individual Nanoparticles in Dispersion Using Size-Tunable Pore Sensors', *ACS Nano*, **6**, 6990–6997 (2012).

31. M. Langecker, V. Arnaut, T.G. Martin, J. List, S. Renner, M. Mayer, H. Dietz, F.C. Simmel, 'Synthetic Lipid Membrane Channels Formed by Designed DNA Nanostructures', *Science*, **338**, 932–936 (2012).

32. D.H. Stoloff, M. Wanunu, 'Recent Trends in Nanopores for Biotechnology', *Curr. Opin. Biotechnol.*, **24**, 699–704 (2013).

33. S. Hernández-Ainsa, K. Misiunas, V.V. Thacker, E.A. Hemmig, U.F. Keyser, 'Voltage-Dependent Properties of DNA Origami Nanopores', *Nano Lett.*, **14**, 1270–1274 (2014).

34. U.F. Keyser, 'Controlling molecular transport through nanopores', *J. R. Soc. Interface*, **63**, 1369–1378 (2011).

35. Y. Song, R. Peng, J. Wang, X. Pan, Y. Sun, D. Li, 'Automatic Particle Detection and Sorting in an Electrokinetic Microfluidic Chip', *Electrophoresis*, **34**, 684–690 (2013).

36. J. Sun, Y. Xianyu, M. Li, W. Liu, L. Zhang, D. Liu, C. Liu, G. Hu, X. Jiang, 'A Microfluidic Origami Chip for Synthesis of Functionalized Polymeric Nanoparticles', *Nanoscale*, **5**, 5262–5265 (2013).

37. B.N. Miles, A.P. Ivanov, K.A. Wilson, F. Dogan, D. Japrung, J.B. Edel, 'Single Molecule Sensing with Solid-State Nanopores: Novel Materials, Methods, and Applications', *Chem. Soc. Rev.*, **42**, 15–28 (2013).

38. D.J. Niedzwiecki, M.M. Mohammad, L. Movileanu, 'Inspection of the Engineered FhuA ΔC/Δ4L Protein Nanopore by Polymer Exclusion', *Biophys. J.*, **103**, 2115–2124 (2012).

39. I. Vodyanoy, S.M. Bezrukov, V.A. Parsegian, 'Probing Alamethicin Channels with Water-Soluble Polymers. Size-modulated osmotic action', *Biophys. J.*, **65**, 2097–2105 (1993).

40. S.M. Bezrukov, 'Ion Channels as Molecular Coulter Counters to Probe Metabolite Transport', *J. Membr. Biol.*, **174**, 1–13 (2000).

41. J.C. Behrends, 'Evolution of the Ion Channel Concept: The Historical Perspective', *Chem. Rev.*, **112**, 6218–6226 (2012).

42. M. Montal, P. Mueller, 'Formation of Bimolecular Membranes from Lipid Monolayers and a Study of Their Electrical Properties', *Proc. Natl. Acad. Sci. U. S. A.*, **69**, 3561–3566 (1972).

43. G. Menestrina, M. Dalla Serra, G. Prévost, 'Mode of Action of β-Barrel Pore-Forming Toxins of the Staphylococcal α-Hemolysin Family', *Toxicon*, **39**, 1661–1672 (2001).

44. S. Howorka, Z. Siwy, 'Nanopore Analytics: Sensing of Single Molecules', *Chem. Soc. Rev.*, **38**, 2360–2384 (2009).

45. H.-C. Wu, Y. Astier, G. Maglia, E. Mikhailova, H. Bayley, 'Protein Nanopores with Covalently Attached Molecular Adapters', *J. Am. Chem. Soc.*, **129**, 16142–16148 (2007).

46. G. Baaken, N. Ankri, A.-K. Schuler, J. Rühe, J.C. Behrends, 'Nanopore-Based Single-Molecule Mass Spectrometry on a Lipid Membrane Microarray', *ACS Nano*, **5**, 8080–8088 (2011).

47. E. Campos, C.E. McVey, R.P. Carney, F. Stellacci, Y. Astier, J. Yates, 'Sensing Single Mixed-Monolayer Protected Gold Nanoparticles by the α-Hemolysin Nanopore', *Anal. Chem.*, **85**, 10149–10158 (2013).

48. A. Liu, Q. Zhao, X. Guan, 'Stochastic Nanopore Sensors for the Detection of Terrorist Agents: Current Status and Challenges', *Anal. Chim. Acta*, **675**, 106–115 (2010).

49. D. Wang, Q. Zhao, R.S.S.d. Zoysa, X. Guan, 'Detection of Nerve Agent Hydrolytes in an Engineered Nanopore', *Sens. Actuators B*, **139**, 440–446 (2009).

50. X. Guan, L.-Q. Gu, S. Cheley, O. Braha, H. Bayley, 'Stochastic Sensing of TNT with a Genetically Engineered Pore', *ChemBioChem*, **6**, 1875–1881 (2005).

51. A. Asandei, A. Apetrei, T. Luchian, 'Uni-Molecular Detection and Quantification of Selected β-Lactam Antibiotics with a Hybrid α-Hemolysin Protein Pore', *J. Mol. Recognit.*, **24**, 199–207 (2011).

52. H. Bayley, P.S. Cremer, 'Stochastic Sensors Inspired by Biology', *Nature*, **413**, 226–230 (2001).

53. T.Z. Butler, M. Pavlenok, I.M. Derrington, M. Niederweis, J.H. Gundlach, 'Single-Molecule DNA Detection with an Engineered MspA Protein Nanopore', *Proc. Natl. Acad. Sci. U.S.A.*, **105**, 20647–20652 (2008).

54. R.D. Maitra, J. Kim, W.B. Dunbar, 'Recent Advances in Nanopore Sequencing', *Electrophoresis*, **33**, 3418–3428 (2012).

55. S. Majd, E.C. Yusko, Y.N. Billeh, M.X. Macrae, J. Yang, M. Mayer, 'Applications of Biological Pores in Nanomedicine, Sensing, and Nanoelectronics', *Curr. Opin. Biotechnol.*, **21**, 439–476 (2010).

56. L. Song, M.R. Hobaugh, C. Shustak, S. Cheley, H. Bayley, J.E. Gouaux, 'Structure of Staphylococcal Alpha-Hemolysin, a Heptameric Transmembrane Pore', *Science*, **274**, 1859–1866 (1996).

57. E. Campos, *A Nanopore-based Stochastic Detection Method: Single Molecule Characterisation of Nanoparticles Using α-Hemolysin*, Universidade Nova de Lisboa, Lisboa, Portugal, 2013.

58. *The PyMOL Molecular Graphics System*, Version 1.4.1, Schrödinger, LLC, 2011.

59. S.M. Bezrukov, I. Vodyanoy, 'Probing Alamethicin Channels with Water-soluble Polymers. Effect on Conductance of Channel States', *Biophys. J.*, **64**, 16–25 (1993).

60. Oxford Nanopore Technologies® https://www.nanoporetech.com

61. M. Mayer, J.K. Kriebel, M.T. Tosteson, G.M. Whitesides, 'Microfabricated Teflon Membranes for Low-Noise

62. M. Hashemi, S. Achenbach, B. Moazed, D. Klymyshyn, 'PMMA Polymer Membrane-Based Single Cylindrical Submicron Pores: Electrical Characterization and Investigation of Their Applicability in Resistive-Pulse Biomolecule Detection', *Am. J. Anal. Chem.*, **3**, 534–543 (2012).

63. J. Li, D. Stein, C. McMullan, D. Branton, M.J. Aziz, J.A. Golovchenko, 'Ion-Beam Sculpting at Nanometre Length Scales', *Nature*, **412**, 166–169 (2001).

64. M. Wanunu, A. Meller, 'Chemically Modified Solid-State Nanopores', *Nano Lett.*, **7**, 1580–1585 (2007).

65. A.J. Storm, J.H. Chen, X.S. Ling, H.W. Zandbergen, C. Dekker, 'Fabrication of Solid-State Nanopores with Single-Nanometre Precision', *Nat. Mater.*, **2**, 537–540 (2003).

66. H. Shadpour, H. Musyimi, J. Chen, S.A. Soper, 'Physiochemical Properties of Various Polymer Substrates and their Effects on Microchip Electrophoresis Performance', *J. Chromatogr. A*, **1111**, 238–251 (2006).

67. M. Sridhar, D. Xu, Y. Kang, A.B. Hmelo, L.C. Feldman, D. Li, D. Li, 'Experimental Characterization of a Metal-Oxide-Semiconductor Field-Effect Transistor-Based Coulter Counter', *J. Appl. Phys.*, **103**, 104701-1–104701-10 (2008).

68. M. Ali, R. Neumann, W. Ensinger, 'Sequence-Specific Recognition of DNA Oligomer Using Peptide Nucleic Acid (PNA)-Modified Synthetic Ion Channels: PNA/DNA Hybridization in Nanoconfined Environment', *ACS Nano*, **4**, 7267–7274 (2010).

69. S.M. Iqbal, D. Akin, R. Bashir, 'Solid-State Nanopore Channels with DNA Selectivity', *Nat. Nanotechnol.*, **2**, 243–248 (2007).

70. B. Yameen, M. Ali, R. Neumann, W. Ensinger, W. Knoll, O. Azzaroni, 'Ionic Transport Through Single Solid-State Nanopores Controlled with Thermally Nanoactuated Macromolecular Gates', *Small*, **5**, 1287–1291 (2009).

71. M. Wanunu, W. Morrison, Y. Rabin, A.Y. Grosberg, A. Meller, 'Electrostatic Focusing of Unlabelled DNA into Nanoscale Pores Using a Salt Gradient', *Nat. Nanotechnol.*, **5**, 160–165 (2010).

72. U.F. Keyser, S. van Dorp, S.G. Lemay, 'Tether Forces in DNA Electrophoresis', *Chem. Soc. Rev.*, **39**, 939–947 (2010).

73. E. Beamish, H. Kwok, V. Tabard-Cossa, M. Godin, 'Fine-tuning the Size and Minimizing the Noise of Solid-state Nanopores', *J. Vis. Exp.*, e51081 (2013).

74. R.M. Smeets, U.F. Keyser, N.H. Dekker, C. Dekker, 'Noise in Solid-State Nanopores', *Proc. Natl. Acad. Sci. U.S.A.*, **105**, 417–421 (2008).

75. J.K. Rosenstein, M. Wanunu, C.A. Merchant, M. Drndic, K.L. Shepard, 'Integrated Nanopore Sensing

Platform with Sub-Microsecond Temporal Resolution', *Nat. Methods*, **9**, 487–492 (2012).

76. R.M. Smeets, N.H. Dekker, C. Dekker, 'Low-Frequency Noise in Solid-State Nanopores', *Nanotechnology*, **20**, 095501 (2009).

77. D.J. Niedzwiecki, J. Grazul, L. Movileanu, 'Single-Molecule Observation of Protein Adsorption onto an Inorganic Surface', *J. Am. Chem. Soc.*, **132**, 10816–10822 (2010).

78. S. Garaj, W. Hubbard, A. Reina, J. Kong, D. Branton, J.A. Golovchenko, 'Graphene as a Subnanometre Trans-Electrode Membrane', *Nature*, **467**, 190–193 (2010).

79. G.F. Schneider, S.W. Kowalczyk, V.E. Calado, G. Pandraud, H.W. Zandbergen, L.M. Vandersypen, C. Dekker, 'DNA Translocation through Graphene Nanopores', *Nano Lett.*, **10**, 3163–3167 (2010).

80. S.M. Avdoshenko, D. Nozaki, C. Gomes da Rocha, J.W. González, M.H. Lee, R. Gutierrez, G. Cuniberti, 'Dynamic and Electronic Transport Properties of DNA Translocation through Graphene Nanopores', *Nano Lett.*, **13**, 1969–1976 (2013).

81. F. Traversi, C. Raillon, S.M. Benameur, K. Liu, S. Khlybov, M. Tosun, D. Krasnozhon, A. Kis, A. Radenovic, 'Detecting the Translocation of DNA Through a Nanopore Using Graphene Nanoribbons', *Nat. Nanotechnol.*, **8**, 939–945 (2013).

82. S.C. O'Hern, C.A. Stewart, M.S.H. Boutilier, J.-C. Idrobo, S. Bhaviripudi, S.K. Das, J. Kong, T. Laoui, M. Atieh, R. Karnik, 'Selective Molecular Transport through Intrinsic Defects in a Single Layer of CVD Graphene', *ACS Nano*, **6**, 10130–10138 (2012).

83. Y.P. Shan, P.B. Tiwari, P. Krishnakumar, I. Vlassiouk, W.Z. Li, X.W. Wang, Y. Darici, S.M. Lindsay, H.D. Wang, S. Smirnov, J. He, 'Surface Modification of Graphene Nanopores for Protein Translocation', *Nanotechnology*, **24**, 495102 (2013).

84. H.W.C. Postma, 'Rapid Sequencing of Individual DNA Molecules in Graphene Nanogaps', *Nano Lett.*, **10**, 420–425 (2010).

85. M. Venkatesan, D. Estrada, S. Banerjee, X. Jin, V.E. Dorgan, M.-H. Bae, N.R. Aluru, E. Pop, R. Bashir, 'Stacked Graphene-Al2O3 Nanopore Sensors for Sensitive Detection of DNA and DNA–Protein Complexes', *ACS Nano*, **6**, 441–450 (2011).

86. L. Sun, R.M. Crooks, 'Single Carbon Nanotube Membranes: A Well-Defined Model for Studying Mass Transport through Nanoporous Materials', *J. Am. Chem. Soc.*, **122**, 12340–12345 (2000).

87. V. Lulevich, S. Kim, C.P. Grigoropoulos, A. Noy, 'Frictionless Sliding of Single-Stranded DNA in a Carbon Nanotube Pore Observed by Single Molecule Force Spectroscopy', *Nano Lett.*, **11**, 1171–1176 (2011).

88. Y. Rudzevich, Y. Lin, A. Wearne, A. Ordonez, O. Lupan, L. Chow, 'Characterization of Liposomes and Silica Nanoparticles Using Resistive Pulse Method', *Colloids Surf. A Physicochem. Eng. Asp.*, **448**, 9–15 (2014).

89. Y. Wang, K. Kececi, M.V. Mirkin, V. Mani, N. Sardesai, J.F. Rusling, 'Resistive-Pulse Measurements with Nanopipettes: Detection of Au Nanoparticles and Nanoparticle-Bound Anti-Peanut IgY', *Chem. Sci.*, **4**, 655–663 (2013).

90. P. Actis, A.C. Mak, N. Pourmand, 'Functionalized Nanopipettes: Toward Label-Free, Single Cell Biosensors', *Bioanal. Rev.*, **1**, 177–185 (2010).

91. L.J. Steinbock, O. Otto, C. Chimerel, J. Gornall, U.F. Keyser, 'Detecting DNA Folding with Nanocapillaries', *Nano Lett.*, **10**, 2493–2497 (2010).

92. L.T. Sexton, L.P. Horne, C.R. Martin, 'Developing Synthetic Conical Nanopores for Biosensing Applications', *Mol. Biosyst.*, **3**, 667–685 (2007).

93. G.S. Roberts, D. Kozak, W. Anderson, M.F. Broom, R. Vogel, M. Trau, 'Tunable Nano/Micropores for Particle Detection and Discrimination: Scanning Ion Occlusion Spectroscopy', *Small*, **6**, 2653–2658 (2010).

94. G.R. Willmott, M.F. Broom, M.L. Jansen, R.M. Young, W.M. Arnold, '*Tunable Elastomeric Nanopores*', in *Molecular- and Nano-Tubes*, eds O. Hayden, K. Nielsch, Springer, Berlin, 209–261, 2011.

95. R. Vogel, G. Willmott, D. Kozak, G.S. Roberts, W. Anderson, L. Groenewegen, B. Glossop, A. Barnett, A. Turner, M. Trau, 'Quantitative Sizing of Nano/Microparticles with a Tunable Elastomeric Pore Sensor', *Anal. Chem.*, **83**, 3499–3506 (2011).

96. G.R. Willmott, P.W. Moore, 'Reversible Mechanical Actuation of Elastomeric Nanopores', *Nanotechnology*, **19**, 475504 (2008).

97. Izon, http://www.izon.com/products/qnano/qnano.

98. E.R. Billinge, J. Muzard, M. Platt, 'Tunable Resistive Pulse Sensing as a Tool to Monitor Analyte Induced Particle Aggregation', *Nanomater. Nanosci.*, **1**, 1 (2013).

99. A.R. Hall, A. Scott, D. Rotem, K.K. Mehta, H. Bayley, C. Dekker, 'Hybrid Pore Formation by Directed Insertion of α-Haemolysin into Solid-State nanopores', *Nat. Nanotechnol.*, **5**, 874–877 (2010).

100. L. Liu, C. Yang, K. Zhao, J. Li, H.-C. Wu, 'Ultrashort Single-Walled Carbon Nanotubes in a Lipid Bilayer as a New Nanopore Sensor', *Nat. Commun.*, **4**, 2989 (2013).

101. J. Sha, T. Hasan, S. Milana, C. Bertulli, N.A.W. Bell, G. Privitera, Z. Ni, Y. Chen, F. Bonaccorso, A.C. Ferrari, U.F. Keyser, Y.Y.S. Huang, 'Nanotubes Complexed with DNA and Proteins for Resistive-Pulse Sensing', *ACS Nano*, **7**, 8857–8869 (2013).

102. G. Wang, B. Zhang, J.R. Wayment, J.M. Harris, H.S. White, 'Electrostatic-Gated Transport in Chemically

Q5

Modified Glass Nanopore Electrodes', *J. Am. Chem. Soc.*, **128**, 7679–7686 (2006).

103. R. Wei, T.G. Martin, U. Rant, H. Dietz, 'DNA Origami Gatekeepers for Solid-State Nanopores', *Angew. Chem. Int. Ed. Engl.*, **51**, 4864–4867 (2012).

104. J.R. Burns, K. Gopfrich, J.W. Wood, V.V. Thacker, E. Stulz, U.F. Keyser, S. Howorka, 'Lipid-Bilayer-Spanning DNA Nanopores with a Bifunctional Porphyrin Anchor', *Angew. Chem. Int. Ed. Engl.*, **52**, 12069–12072 (2013).

105. N.A.W. Bell, C.R. Engst, M. Ablay, G. Divitini, C. Ducati, T. Liedl, U.F. Keyser, 'DNA Origami Nanopores', *Nano Lett.*, **12**, 512–517 (2011).

106. H. Daiguji, P. Yang, A. Majumdar, 'Ion Transport in Nanofluidic Channels', *Nano Lett.*, **4**, 137–142 (2003).

107. R. Karnik, K. Castelino, C. Duan, A. Majumdar, 'Diffusion-Limited Patterning of Molecules in Nanofluidic Channels', *Nano Lett.*, **6**, 1735–1740 (2006).

108. U.D. Larsen, G. Blankenstein, J. Branebjerg *Microchip Coulter Particle Counter*, Solid State Sensors and Actuators, 1997. TRANSDUCERS '97 Chicago., International Conference on 16–19 Jun 1997, vol. **1312**, 1319–1322, 1997.

109. M. Koch, A.G.R. Evans, A. Brunnschweiler, 'Design and Fabrication of a Micromachined Coulter Counter', *J. Micromech. Microeng.*, **9**, 159–161 (1999).

110. K. Roberts, M. Parmeswaran, M. Moore, R. S. Muller, A Silicon Microfabricated Aperture for Counting Cells Using the Aperture Impedance Technique. Electrical and Computer Engineering, 1999 IEEE Canadian Conference on 9–12 May 1999, vol. **1663**, 1668–1673, 1999.

111. O.A. Saleh, L.L. Sohn, 'An Artificial Nanopore for Molecular Sensing', *Nano Lett.*, **3**, 37–38 (2002).

112. O.A. Saleh, L.L. Sohn, 'Quantitative Sensing of Nanoscale Colloids Using a Microchip Coulter Counter', *Rev. Sci. Instrum.*, **72**, 4449–4451 (2001).

113. O.A. Saleh, L.L. Sohn, 'Direct Detection of Antibody–Antigen Binding Using an On-Chip Artificial Pore', *Proc. Natl. Acad. Sci. U.S.A.*, **100**, 820–824 (2003).

114. O.A. Saleh, L.L. Sohn, '*An On-Chip Artificial Pore for Molecular Sensing*', in *BioMEMS and Biomedical Nanotechnology*, eds M. Ferrari, R. Bashir, S. Wereley, Springer, New York, 35–53, 2007.

115. O.A. Saleh, L.L. Sohn, 'Correcting Off-Axis Effects in an On-Chip Resistive-Pulse Analyzer', *Rev. Sci. Instrum.*, **73**, 4396–4398 (2002).

116. Z. Zhang, J. Zhe, S. Chandra, J. Hu, 'An Electronic Pollen Detection Method Using Coulter Counting Principle', *Atmos. Environ.*, **39**, 5446–5453 (2005).

117. A.V. Jagtiani, R. Sawant, J. Zhe, 'A Label-Free High Throughput Resistive-Pulse Sensor for Simultaneous Differentiation and Measurement of Multiple Particle-Laden Analytes', *J. Micromech. Microeng.*, **16**, 1530–1539 (2006).

118. R. Rodriguez-Trujillo, O. Castillo-Fernandez, M. Garrido, M. Arundell, A. Valencia, G. Gomila, 'High-Speed Particle Detection in a Biosens Bioelectronmicro-Coulter Counter with Two-Dimensional Adjustable Aperture', *Biosens. Bioelectron.*, **24**, 290–296 (2008).

119. J.H. Nieuwenhuis, J. Bastemeijer, P.M. Sarro, M.J. Vellekoop, 'Integrated Flow-Cells for Novel Adjustable Sheath Flows', *Lab Chip*, **3**, 56–61 (2003).

120. R. Rodriguez-Trujillo, C.A. Mills, J. Samitier, G. Gomila, 'Low Cost Micro-Coulter Counter with Hydrodynamic Focusing', *Microfluid. Nanofluid.*, **3**, 171–176 (2007).

121. R. Scott, P. Sethu, C.K. Harnett, 'Three-Dimensional Hydrodynamic Focusing in a Microfluidic Coulter Counter', *Rev. Sci. Instrum.*, **79**, 046104 (2008).

122. P. Paiè, F. Bragheri, R.M. Vazquez, R. Osellame, 'Straightforward 3D Hydrodynamic Focusing in Femtosecond Laser Fabricated Microfluidic Channels', *Lab Chip*, **14**, 1826–1833 (2014).

123. J. Riordon, M. Mirzaei, M. Godin, 'Microfluidic Cell Volume Sensor with Tunable Sensitivity', *Lab Chip*, **12**, 3016–3019 (2012).

124. A. Carbonaro, L.L. Sohn, 'A Resistive-Pulse Sensor Chip for Multianalyte Immunoassays', *Lab Chip*, **5**, 1155–1160 (2005).

125. V.J. Ashish, Z. Jiang, H. Jun, C. Joan, 'Detection and Counting of Micro-Scale Particles and Pollen using a Multi-Aperture Coulter Counter', *Meas. Sci. Technol.*, **17**, 1706 (2006).

126. D. Xu, Y. Kang, M. Sridhar, A.B. Hmelo, L.C. Feldman, D. Li, D. Li, 'Wide-Spectrum, Ultrasensitive Fluidic Sensors with Amplification from both Fluidic Circuits and Metal Oxide Semiconductor Field Effect Transistors', *Appl. Phys. Lett.*, **91**, 013901 (2007).

127. X. Wu, Y. Kang, Y.N. Wang, D. Xu, D. Li, 'Microfluidic Differential Resistive Pulse Sensors', *Electrophoresis*, **29**, 2754–2759 (2008).

128. S. Song, S. Choi, 'Design Rules for Size-Based Cell Sorting and Sheathless Cell Focusing by Hydrophoresis', *J. Chromatogr. A*, **1302**, 191–196 (2013).

129. J. Riordon, M. Nash, M. Calderini, M. Godin, 'Using Active Microfluidic Flow Focusing to Sort Particles and Cells Based on High-Resolution Volume Measurements', *Microelectron. Eng.*, **118**, 35–40 (2014).

130. R.W. DeBlois, C.P. Bean, R.K.A. Wesley, 'Electrokinetic Measurements with Submicron Particles and Pores by the Resistive Pulse Technique', *J. Colloid Interface Sci.*, **61**, 323–335 (1977).

131. G.S. Roberts, S. Yu, Q. Zeng, L.C. Chan, W. Anderson, A.H. Colby, M.W. Grinstaff, S. Reid, R. Vogel, 'Tunable

Pores for Measuring Concentrations of Synthetic and Biological Nanoparticle Dispersions', *Biosens. Bioelectron.*, **31**, 17–25 (2012).

132. L. Yang, M.F. Broom, I.G. Tucker, 'Characterization of a Nanoparticulate Drug Delivery System using Scanning Ion Occlusion Sensing', *Pharm. Res.*, **29**, 2578–2586 (2012).

133. W. Anderson, D. Kozak, V.A. Coleman, Å.K. Jämting, M. Trau, 'A Comparative Study of Submicron Particle Sizing Platforms: Accuracy, Precision and Resolution Analysis of Polydisperse Particle Size Distributions', *J. Colloid Interface Sci.*, **405**, 322–330 (2013).

134. N.C. Bell, C. Minelli, J. Tompkins, M.M. Stevens, A.G. Shard, 'Emerging Techniques for Submicrometer Particle Sizing Applied to Stöber Silica', *Langmuir*, **28**, 10860–10872 (2012).

135. M. Figueiredo, 'Sizing Nanoparticles in Liquids: An Overview of Methods', in *Drug Delivery Systems: Advanced Technologies Potentially Applicable in Personalised Treatment*, ed. J. Coelho, Springer, Netherlands, 87–107, Vol. **4**, 2013.

136. O.A. Saleh, *A Novel Resistive Pulse Sensor for Biological Measurements*, Princeton University, Princeton, NJ, 2003.

137. S. Zheng, Y.C. Tai, In Design and Fabrication of a Micro Coulter Counter with Thin Film Electrodes, Proceedings of the 4th Annual International IEEE EMBS Special Topic Conference on Microtechnologies in Medicine and Biology (IEEE-EMBS/MMB2005), Bankoku-Shinryokan, Okinawa, JAPAN, 2006; Bankoku-Shinryokan, Okinawa, JAPAN, 16–19, 2006.

138. E. Campos, A. Asandei, C.E. McVey, J.C. Dias, A.S.F. Oliveira, C.M. Soares, T. Luchian, Y. Astier, 'The Role of Lys147 in the Interaction Between MPSA-Gold Nanoparticles and the α-Hemolysin Nanopore', *Langmuir*, **28**, 15643–15650 (2012).

QUERIES TO BE ANSWERED BY AUTHOR (SEE MARGINAL MARKS Q..)

IMPORTANT NOTE: You may answer these queries by email. If you prefer, you may print out the PDF, and mark your corrections and answers directly on the proof at the relevant place. Do NOT mark your corrections on this query sheet. Please see the proofing instructions for information about how to return your corrections and query answers.

Q1. As references 18 and 21 are identical, 21 has been replaced with 18 and subsequent references have been renumbered to maintain sequence in the text.

Q2. As per style, a Related Articles Section containing a list of articles that the reader could cross refer should be present. Please provided a list of articles from the master list enclosed.

Q3. Please provide the year of publication, title and accessed date for Reference 60.

Q4. Please provide the volume number for Reference 73.

Q5. Please provide the year of publicaion, title and accessed date for Reference 97.